Mobility Prediction Based Joint Stable Routing and Channel Assignment for Mobile Ad Hoc Cognitive Networks

Feilong Tang, Minyi Guo, *Senior Member, IEEE*, Song Guo, *Member, IEEE*, and Cheng-Zhong Xu, *Fellow, IEEE*

Abstract—Link instability and channel interference cause significant performance degradation to mobile ad hoc cognitive networks (MACNets). Existing work designs routing and assigns channels separately or does not consider mobility prediction and channel vacation to primary nodes. In this paper, we investigate how to jointly optimize route setup and channel assignment. Firstly, we propose an *integrated data transmission cost (IDTC)* to quantitatively measure the communication quality of links. This novel routing metric *IDTC* integratively considers 1) node mobility, 2) co-channel interference among primary and cognitive nodes, 3) relay workload on a specified channel, and 4) distance between the relay and the destination node. We, then, design channel assignment algorithms that completely avoid the interference with primary nodes and minimize the conflict to cognitive nodes. Finally, we propose a joint stable routing and channel assignment (J-SRCA) protocol based on mobility prediction for the network throughput maximization. In our J-SRCA, each link selected hop by hop is simultaneously assigned an interference-avoiding channel during a route setup. NS2-based simulation results demonstrate that our J-SRCA significantly improves various network performance, and the higher interference degree cognitive networks experience, the more improvement our J-SRCA will bring to the networks.

Index Terms—Cognitive network, stable routing, channel assignment, mobility model, multi-hop ad hoc network

1 Introduction

Cognitive networks can partly solve the spectrum scarcity problem through dynamic spectrum access [1], where cognitive nodes (CNs) can dynamically sense and opportunistically employ unused spectrum licensed to primary nodes (PNs). A CN, however, has to immediately vacate the channel when the corresponding PN activates again [2].

The stable routing is a fundamental issue in mobile ad hoc cognitive networks (MACNets) because the network performance highly depends on the stability of routes selected by routing protocols [5], [6]. The link stability in MACNets suffers from node mobility and channel interference with not only CNs but also PNs. In MACNets, frequently changing PN activities and node mobility make available channels of CNs changing over time and over locations [3]. A ''stable route'' selected only in terms of mobility may become unavailable soon due to the communication of adjacent PNs and CNs. Further, stable routing in multi-hop multi-flow MACNets becomes even worse because multiple links potentially interfere with each other. Therefore, routing and channel assignment in MACNets should be jointly designed and optimized [2], [4] together with the node mobility prediction.

In this paper, we propose a *joint stable routing and channel assignment (J-SRCA)* protocol based on the mobility prediction to solve the above challenging issues. For the route selection, we focus on making a path available as long as possible. For the channel assignment, we consider an optimal solution that completely avoids the impact to PNs and at the same time, mitigates both intra- and inter-flow interferences among CNs. Compared with existing schemes, our approach significantly improves system performance in mobile cognitive environments, through comprehensively considering the mobility prediction and cross-layer design. To the best of our knowledge, this is the first paper that has addressed the J-SRCA problem in multi-channel multi-flow mobile cognitive networks. Main contributions of this paper are summarized as follows.

(1) We formally define the *joint stable routing and channel assignment (J-SRCA)* problem. The objective of the J-SRCA problem is to maximize system throughput of multi-hop multi-channel multi-flow MACNets.
(2) We propose a new *integrated data transmission cost (IDTC)* to quantitatively measure the communication quality of links. It considers not only the path stability that suffers from node mobility, unexpected PN activities, co-channel interference among inter- and intra-flows, but also path length and relay workload on the assigned channel.
(3) We propose and implement a novel distributed and cross-layer protocol *J-SRCA*, which reside between

- *F. Tang and M. Guo are with the Department of Computer Science and Engineering, Shanghai Jiao Tong University, Shanghai 200240, China. E-mail: {tang-fl, guo-my}@cs.sjtu.edu.cn.*
- *S. Guo is with the School of Computer Science, The University of Aizu, Fukushima 965-8580, Japan. E-mail: sguo@u-aizu.ac.jp.*
- *C.-Z. Xu is with the Department of Electrical and Computer Engineering, Wayne State University, USA, and Shenzhen Institutes of Advanced Technology (SIAT) of Chinese Academy of Sciences, China. E-mail: czxu@wayne.edu.*

Manuscript received 2 June 2013; revised 5 Aug. 2013; accepted 6 Aug. 2013. Date of publication 25 Aug. 2013; date of current version 12 Feb. 2016. Recommended for acceptance by X.-Y. Li.
For information on obtaining reprints of this article, please send e-mail to: reprints@ieee.org, and reference the Digital Object Identifier below.
Digital Object Identifier no. 10.1109/TPDS.2013.216

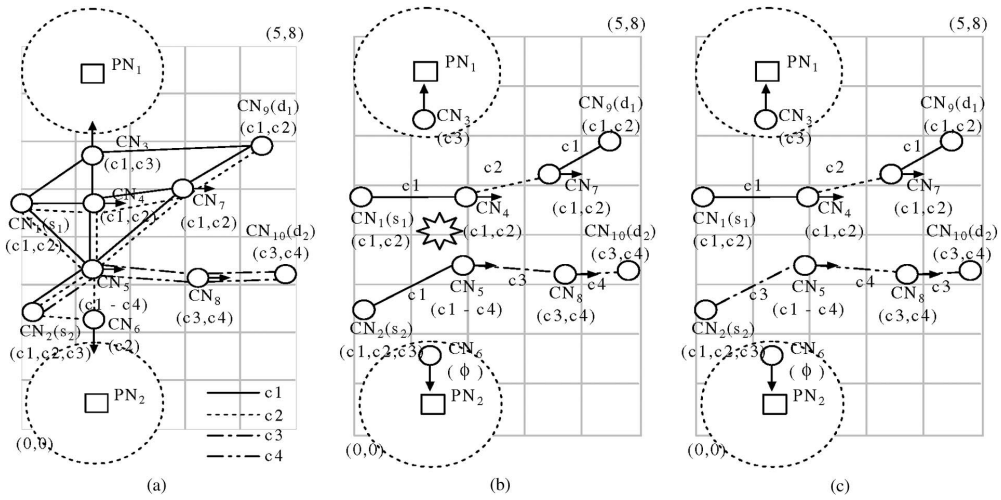

Fig. 1. Motivating scenario for J-SRCA. (a) Initial topology. (b) only stable routing. (c) joint stable routing and channel assignment.

MAC and network layers, to coordinate stable route selection and interference-avoiding channel assignment. The J-SRCA protocol is built on our transmission cost model IDTC, channel assignment algorithms and geography information.

(4) Our approach minimizes the channel interference. Any link that potentially impacts PNs due to lack of available channel is completely excluded by our J-SRCA protocol. Moreover, our J-SRCA pays higher priority to avoiding the inter-flow interference than the intra-flow interference.

The remainder of this paper is organized as follows. In Section 2, we describe a motivated scenario. Section 3 presents the network model, formalizes the J-SRCA problem and proposes a channel interference model. In Section 4, we present a stability prediction model and a routing measure metric *IDTC*, and propose the channel assignment algorithms and J-SRCA protocol. We systematically examine our approach by testing and evaluating the J-SRCA with related proposals using NS2-based simulation system in Section 5. Section 6 briefly reviews related work. Section 7 concludes this paper.

2 Scenario and Motivation

We illustrate the significance of our J-SRCA protocol through the following scenario, shown in Fig. 1. Each CN has a set of available channels marked below the node. CN_5 with the mark ''(c1-c4)'', e.g., may use channel set {c1, c2, c3, c4}. PN_1 and PN_2 are using their licensed channels c1 and c2, respectively. CN_4, CN_5, CN_7 and CN_8 move eastwardly at the speed of 1 m/s; and CN_3 and CN_6 move towards PN_1 and PN_2 at the speed of 0.5 m/s, respectively. There are two data flows: flow 1 from CN_1 to CN_9 while flow 2 from CN_2 to CN_{10}. Note that four kinds of lines denote four different channels.

Initial network topology is illustrated in Fig. 1a. Intuitively, CN_1 can select any of three nodes: CN_3, CN_4 and CN_5 as the next hop and there are three candidate paths: $P_1 = (CN_1 \rightarrow CN_3 \rightarrow CN_9)$, $P_2 = (CN_1 \rightarrow CN_4 \rightarrow CN_7 \rightarrow CN_9)$ and $P_3 = (CN_1 \rightarrow CN_5 \rightarrow CN_7 \rightarrow CN_9)$. After 10 seconds, however, CN_3 enters into the range of PN_1 and CN_5 moves out of the radio range of CN_1, shown in Fig. 1b. For simplicity, we assume that the interference range of each radio is almost equal to its transmission range in this specific scenario. As a result, P_1 can work within only 10 s because CN_3 will interfere with PN_1. Similarly, P_3 also will become unavailable after 10 s because CN_5 moves out of the radio range of CN_1. Comparatively, P_2 potentially is the most stable among $\ell_{1,3}$, $\ell_{1,4}$ and $\ell_{1,5}$, where $\ell_{i,j}$ represents the link between CN_i and CN_j. So, a routing setup should select the links with longer duration. Based on such the principle, CN_1 and CN_2 select CN_4 and CN_5 as their next hops, respectively. On the other hand, according to the routing protocol proposed in [3], a path chosen in multi-radio networks should satisfy higher channel diversity in the path.

After integrating the above two regulations, flow 1 selects path $P_2 = (CN_1 \xrightarrow{c1} CN_4 \xrightarrow{c2} CN_7 \xrightarrow{c1} CN_9)$; and flow 2 selects path $P_4 = (CN_2 \xrightarrow{c1} CN_5 \xrightarrow{c3} CN_8 \xrightarrow{c4} CN_{10})$, where marks above arrows represent the channels used by the corresponding links. Unfortunately, there is a channel interference, marked with a star in Fig. 1b, between $\ell_{1,4}$ and $\ell_{2,5}$ in this routing scheme. We assume that the two flows transmit packets at the link capacities 72.2 Mb/s. As a result, the aggregated network throughput is about $72.2 \times (1/2) + 72.2 \times (1/2) = 72.2$ Mb/s.

To further improve the network throughput, we reassign the channel c3 to $\ell_{2,5}$ and adjust channels of $\ell_{5,8}$ and $\ell_{8,10}$ to c4 and c3 respectively, as shown in Fig. 1c. Now, the aggregated network throughput is maximized to $72.2 + 72.2 = 144.4$ Mb/s. In summary, this scenario demonstrates that routing in MACNets should jointly considers 1) link stability prediction, and 2) co-channel interference with both PNs and CNs in intra- and inter-flows, to improve the network throughput.

3 Network Model and Problem Statement

We firstly present a network model, and then formulate the J-SRCA problem. Finally, we propose the channel interference model in MACNets.

3.1 Network Model

We model a MACNet as an undirected graph $G = (V, E)$, where V is the union of the CN set (V_C) and the PN set (V_P)

such that $\mathrm{V} = \mathrm{V}_C \bigcup \mathrm{V}_P$; E is the union of E_C and E_P (the set of links among CNs and PNs, respectively) such that $E = E_C \bigcup E_P$. Each CN $u \in V_C$ is equipped with q cognitive radios, as well as a traditional wireless interface, which forms a common control channel (CCC) to transmit control messages, such as routing packets. The CCC does not interfere with any data channels.

We divide continuous time as a series of discrete time slots. The available data channel set of a CN u is described as $\mathrm{C}_u(t) = \{c_i^u | i = 1, 2, \ldots, c_u(t)\}$ in a time slot t. A pair of CNs u and v can communicate only on a common channel $c_{u,v}(t) \in_{u,v} (t) = \mathrm{C}_u(\mathrm{t}) \bigcap \mathrm{C}_v(\mathrm{t})$. Note that 1) any two channels c_i and c_j $(i \neq j)$ are orthogonal; and 2) although $C_u(t)$ changes over time, we assume that $C_u(t)$ is constant during a time slot t.

For any pair of $u, v \in V_C$, we used $\mathrm{d}_{u,v}(\mathrm{t}) = \|u - v\|$ to denote the euclidean distance between u and v in a time slot t. A link $\ell_{u,v}$ is available only if $\|\mathrm{C}_{u,v}(\mathrm{t})\| \geq 1$ and $\mathrm{d}_{u,v}(\mathrm{t}) \leq \mathrm{R}_T$, where $\|\mathrm{C}_{u,v}(\mathrm{t})\|$ refers to the number of data channels in $C_{u,v}(t)$; and R_T is the transmission range of a CN. In this case, u and v can communicate with each other. Finally, two link-channels $\ell_{u,v}^c$ and $\ell_{u',v'}^{c'}$ interfere with each other during a time slot t, marked as $\ell_{u,v}^c \otimes \ell_{u',v'}^{c'}$, if 1) $\mathrm{c} = \mathrm{c}'$; and 2) at least one of $\mathrm{d}_{u,u'}(\mathrm{t})$, $\mathrm{d}_{u,v'}(\mathrm{t})$, $\mathrm{d}_{v,u'}(\mathrm{t})$ and $\mathrm{d}_{v,v'}(\mathrm{t})$ is no more than the interference range R_I.

3.2 J-SRCA Problem

We formulate the J-SRCA problem as follows, where the notations are described in Table 1.

$$\max \quad T = \sum_{k=1}^{K} t_{f_k} \tag{1}$$

$$s.t.:$$

$$IDTC_{f_k}^{\ell_{u,v}^c} \leq IDTC_{f_k}^{\ell_{u,v'}^{c'}},\ \forall u \in V_C;\ \forall v, v' \in N^u;\ \forall c, c' \in C_{u,v}(t) \tag{2}$$

$$c_{u,v}^{f_k}(t) \neq c_{u',v'}^{f_{k'}}(t),\ \forall u, v, u', v' \in V_c; \ell_{u,v}^c \otimes \ell_{u',v'}^c;\ 1 \leqslant k, k' \leqslant K \tag{3}$$

$$\widetilde{\ell}_{u,v}^{c(t)} = \widetilde{\ell}_{v,u}^{c(t)}, \quad \forall u, v \in V_c \tag{4}$$

$$\sum_{k=1}^{K} \sum_{v \in N^u} \sum_{c(t) \in C_{u,v}(t)} c(t) | \widetilde{\ell}_{(u,v):f_k}^{c(t)} = 1 \leq q,\ \forall u \in V_c \tag{5}$$

$$\sum_{k=1}^{K} \sum_{v \in N^u} \sum_{c(t) \in C_{u,v}(t)} \left(\widetilde{\ell}_{(v,u):f_k}^{c(t)} \times t_{v,u}^c + t_u - \widetilde{\ell}_{(u,v):f_k}^{c(t)} \times t_{u,v}^c \right) = 0,\ \forall u \in V_c \tag{6}$$

$$\sum_{k=1}^{K} \sum_{v \in N^u} \sum_{c(t) \in C_u(t)} \left(\widetilde{\ell}_{(u,v):f_k}^{c(t)} \times t_{u,v}^c + \widetilde{\ell}_{(v,u):f_k}^{c(t)} \times t_{v,u}^c \right) \leq w_u,\ \forall u \in V_c. \tag{7}$$

Formula (1) is the optimization objective, i.e., maximizing network throughput, of the J-SRCA problem. Constraint (2) means that during route setup, each node u selects the next hop v with the minimal transmission cost for a flow f_k, which guarantees $\ell_{u,v}$ on channel c is the best next hop in terms of our data transmission cost model *IDTC* in all candidates. Here, both v and v' are 1-hop neighboring nodes of u. Constraint (3) guarantees that assigned channel c for $\ell_{u,v}$ does not cause inter- and intra-flow interferences during any time slot t. Constraint (4) requires any link is bi-directionally symmetrical. (5) guarantees that any node uses at most q channels simultaneously. (6) provides a flow balance for each CN. Finally, (7) ensures the traffic load of u per unit time does not exceed its bandwidth w_u. Note that t in the above formulation refers to time slots for both the path setup and the traffic passing; and a data transmission session can be finished in multiple time slots.

TABLE 1
Notations

Notations	*Description*
f_k	the kth data flow f_k=(s_k, d_k) (1≤k≤K)
$IDTC_{f_k}^{\ell_{u,v}^c}$	data transmission cost of $\ell_{u,v}$ on a channel c for f_k
$\widetilde{\ell}_{u,v}^{c(t)}$	relationship between $\ell_{u,v}$ and a channel c during a slot t $\widetilde{\ell}_{u,v}^{c(t)}$=1 if u and v can communicate on c during t
$\widetilde{\ell}_{(u,v):f_k}^{c(t)}$	relationship between f_k and $\widetilde{\ell}_{u,v}^{c(t)}$ during t. $\widetilde{\ell}_{(u,v):f_k}^{c(t)}$=1 if f_k goes through $\ell_{u,v}$ on a channel c during t
$t_{u,v}^c$	traffic sent from u to v on channel c in an unit of time
t_u	traffic generated by u in an unit of time
$c_{u,v}^{f_k}(t)$	the channel assigned to $\ell_{u,v}$ for f_k during a time slot t
N^u	the set of 1-hop neighboring nodes of u
t_{f_k}	the throughput of f_k

The J-SRCA problem is a mixed nonlinear integer programming problem. In general, it is NP-hard. In this paper, we will propose a heuristic algorithm for solving the above J-SRCA problem through jointly selecting stable route based on mobility prediction and assigning channels in an interference-avoiding way.

3.3 Channel Interference Model

3.3.1 Channel Interference Categories

Our channel assignment scheme prohibits any potential affect to all PNs, and minimizes the interference to CNs that have been assigned channels. We use $P_{s_k}^{d_k}$ to denote the route for f_k. Channels channels assigned to $P_{s_k}^{d_k}$ is the set $C_{s_k}^{d_k} = \{c_{u,v} | u, v \in P_{s_k}^{d_k}, v \in N^u)\}$, where $c_{u,v}$ is the channel assigned to $\ell_{u,v}$ in $P_{s_k}^{d_k}$. To avoid the co-channel interference, only one link can use a given channel within the *k-hop* neighborhood due to $R_I = kR_T$ $(k > 1)$. So, our channel assignment needs to avoid interference with *active nodes*, which involve in (a) data flow(s), within the *k-hop* neighborhood.

Communication in MACNets suffers from both *intra-flow interference* among adjacent active nodes in the same flow and *inter-flow interference* among different concurrent flows. Accordingly, active nodes can be divided as *critical nodes* and *normal nodes*. The critical nodes cause both inter- and intra-flow interferences while normal nodes only interfere with an intra-flow.

Multiple data flows in MACNets may share the same node. To facilitate channel assignment, we classify inter-flow interferences as the following two categories.

- *Disjoint flow interference (DJFI)*. The multiple flows use completely different paths, without any same node. It potentially conflicts with at most $2(k-1)$ links in each inter-flow f_j.

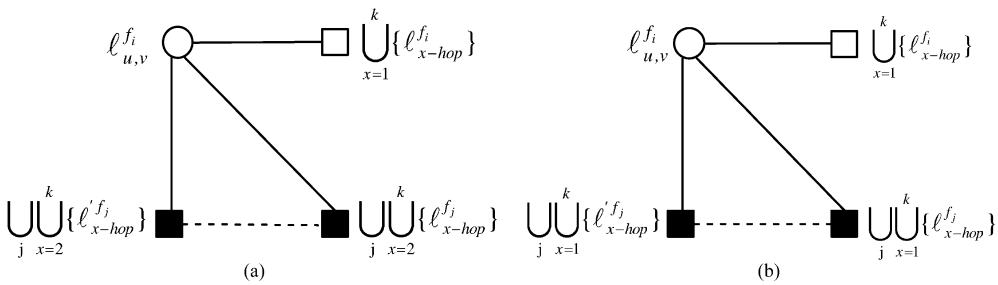

Fig. 2. Interference graph. (a) *DJFI* interference graph. (b) *JFI* interference graph.

- *Joint flow interference (JFI)*. It occurs when multiple flows share an intermediate node. In the worst case, $2k$ links within k hops away from the shared node in each inter-flow f_j will be interfered.

3.3.2 Interference Graph

We propose an *interference graph* to capture interferences among a link $\ell_{u,v}$ in f_i (i.e., $\ell_{u,v}^{f_i}$) and its all $k-hop$ neighboring links, as shown in Fig. 2. In our interference graph, $\ell_{x-hop}^{f_i}$ ($\ell_{x-hop}^{f_j}$) refers to the link, which is x hops away from $\ell_{u,v}$, in f_i (f_j) in the source side. Instead, $\ell_{x-hop}^{'f_j}$ is the counterpart link in the destination side.

In Fig. 2, the white circular nodes will be assigned channels while square nodes have been assigned channels. Specifically, the white square node $\bigcup_{x=1}^{k}\{\ell_{x-hop}^{f_i}\}$ denotes the set of interfered links within k hops in an intra-flow f_i. The black square nodes $\bigcup_j\bigcup_{x=2}^{k}\{\ell_{x-hop}^{f_j}\}$ in Fig. 2a and $\bigcup_j\bigcup_{x=1}^{k}\{\ell_{x-hop}^{f_j}\}$ in Fig. 2b refer to interfered links within k hops in each inter-flow f_j in the source side while $\bigcup_j\bigcup_{x=2}^{k}\{\ell_{x-hop}^{'f_j}\}$ and $\bigcup_j\bigcup_{x=1}^{k}\{\ell_{x-hop}^{'f_j}\}$ are the counterpart in the destination side.

Solid lines in the interference graph reveal potentially interferences among corresponding links while dashed lines means there is no channel interference. Here, we assume that (1) any existing inter-flow f_j has be assigned conflict-free channels and (2)k upstream links (i.e., $\bigcup_{x=1}^{k}\{\ell_{x-hop}^{f_i}\}$) in f_i are also conflict-free. So, the goal of channel assignment is just to remove the potential interferences captured by the solid lines in our interference graph. A ideal channel assignment is to make all the edges in an interference graph become dashed.

4 Mobility Prediction Based Joint Stable Routing and Channel Assignment

This Section presents a link stability prediction model and a new routing metric to quantitatively evaluate the quality of links, then proposes the channel assignment and J-SRCA algorithms.

4.1 Link Stability Prediction

The relative movement between u and v highly impacts the stability of the link $\ell_{u,v}$. In MACNets, it is desirable to keep the connection of a link as long as possible. We use a *maximal lifetime* $MLT_{u,v}$, which refers to the time interval from a route setup to the time when $\ell_{u,v}$ is lost, to measure the stability of $\ell_{u,v}$.

We predict $MLT_{u,v}$ in two stages. Firstly, we assume that node mobility follows the well-known Random Waypoint (RWP) model and calculate maximal duration $T_{u,v}$ of $\ell_{u,v}$. In the second stage, we consider that nodes may arbitrarily change their speed and direction during $T_{u,v}$, and capture the random changes in a probability.

Let each CN be equipped with a GPS and always can communicate with adjacent CNs on the CCC channel using the beacon mechanism. As a result, each CN can easily know the location, the velocity of its 1-hop neighbors. So, we get the distance $d_{u,v}(t)$ as follows.

$$\big(d_{u,v}(t)\big)^2=\Big((x_u(t)-(x_v(t))^2+(y_u(t))-y_v(t)\Big)^2. \quad (8)$$

$\ell_{u,v}$ will lose when $d_{u,v}(t)=R_T$ so that the maximal duration $T_{u,v}$ of $\ell_{u,v}$ can be solved through $d_{u,v}(T_{u,v})=R_T$. Similarly, we can use the following formula to predict the longest duration T_{v,PN_m}, which measures how long v will interfere with any PN_m $(1\le \mathrm{m}\le M)$, through $d_{v,m}(T_{v,PN_m})=R_I$

$$\big(x_v(t)-x_{_{PN_m}}(t)\big)^2+\big(y_v(t)-y_{_{PN_m}}(t)\big)^2=R_I^2. \quad (9)$$

If $T_{u,v}<T_{v,PN_m}$ $(1\le \mathrm{m}\le M)$, the node v will not affect any PN because $\ell_{u,v}$ has lost before it interferes with any PN. So, we only need to consider the case such that $T_{u,v}\ge T_{v,PN_m}$. Existing work, e.g. PCTC [7], prohibits CNs that enter into the interference range of any PN from serving as a relay node. Instead, our approach allows them to be selected as the next hop if they have the orthogonal channel(s) different from the PN(s) affected potentially.

In reality, however, nodes possibly change their velocities at any time, which has been researched in recently years. Probability-based prediction is a category of representative approaches. In this paper, we also use $P(T_{u,v})$, the probability that $\ell_{u,v}$ is available before $T_{u,v}$, to capture such random changes of nodes' velocity. As described in [7], [8], $P(T_{u,v})$ can be estimated in the following formula.

$$P(T_{u,v})\approx e^{-\lambda T_{u,v}e^{-\lambda\tau}}+\zeta(1-e^{-\lambda T_{u,v}}) \quad (10)$$

where λ^{-1} is the mean epoch of nodes; and τ and ζ can be estimated by measurement.

$T_{u,v}$ is the maximum time period that a link can keep if no change in velocities happens. The $P(T_{u,v})$ captures possible changes in velocities that may happen during the period $T_{u,v}$. So, we predict the maximal lifetime $MLT_{u,v}$ of

$\ell_{u,v}$ using the formula (11), which considers random changes in speeds and directions of nodes

$$MLT_{u,v} = T_{u,v} \times P(T_{u,v}). \quad (11)$$

4.2 Routing Metric

In MACNets, the transmission cost of a link $\ell_{u,v}$ depends on

(1) *node mobility*,
(2) *channel interference*,
(3) *workload* of the relay v over a channel c, and
(4) *distance*(d_{v,d_k}) between the relay v and the destination (d_k).

Accordingly, we develop a new transmission cost model, *integrated data transmission cost (IDTC)*, to capture the above factors.

$$IDTC_{f_k}^{\ell_{u,v}} = C_{M+I}^{\ell_{u,v}} \times \left(1 + \frac{b_v^c}{B_v^c}\right) \times \frac{d_{v,d_k}}{d_{u,d_k}}. \quad (12)$$

$IDTC_{f_k}^{\ell_{u,v}}$ is the total data transaction cost of $\ell_{u,v}$ for a flow f_k. $C_{M+I}^{\ell_{u,v}}$ denotes the transmission cost caused by both the node mobility and the channel interference. Moreover, b_v^c in the formula (12) refers to the number of packets in the sending queue for channel c in a relay v; and B_v^c is the total size of the sending queue for c in v. The larger the $\frac{b_v^c}{B_v^c}$ is, the higher the workload in v over c is and the larger $IDTC_{f_k}^{\ell_{u,v}}$ will become. Finally, d_{v,d_k} (d_{u,d_k}) are the distance between the candidate relay v (working node u) and the destination. The closer to the destination the node v is, the less $d_{v,d_k}/d_{u,d_k}$ will become.

Data transmission in MACNets greatly suffers from the node mobility and the channel interference. We formulate $C_{M+I}^{\ell_{u,v}}$ as follows.

$$C_{M+I}^{\ell_{u,v}} = C_M^{\ell_{u,v}} + \alpha C_I^{\ell_{u,v}} \quad (13)$$

where $C_M^{\ell_{u,v}}$ and $C_I^{\ell_{u,v}}$ are the *mobility cost* and *channel interference cost* of $\ell_{u,v}$ caused by the node mobility and the channel interference, respectively; and α is an adjustable coefficient that is used to adjust the weight of the mobility cost and the channel interference cost.

$C_M^{\ell_{u,v}}$ can be estimated using the formula (14). A higher relative movement between u and v will result in a shorter $MLT_{u,v}$. And a link with higher bandwidth can transmit a specified flow within a shorter period of time. On the other hand, we use the formula (15) to capture the cost caused by channel interferences to PNs and CNs.

$$C_M^{\ell_{u,v}} = \frac{\beta}{MLT_{u,v} \times w_{u,v}^c} \quad (14)$$

$$C_I^{\ell_{u,v}} = C_{I:PN}^{\ell_{u,v}} + C_{I:CN}^{\ell_{u,v}} = C_{I:PN}^{\ell_{u,v}} + \sum_{1 \le i \le N} C_{I:CN_i}^{\ell_{u,v}} \quad (15)$$

where $w_{u,v}^c = \min\{w_u^c, w_v^c\}$ is the available bandwidth between u and v; β is an adjustable coefficient; and $C_{I:PN}^{\ell_{u,v}}$, $C_{I:CN}^{\ell_{u,v}}$ and $C_{I:CN_i}^{\ell_{u,v}}$ refer to the interference costs that $\ell_{u,v}$ imposes on all PNs, CNs and CN_i, respectively.

Through the experimental testing, we found that the effective value of the above α and β depends on the node speed; and the more quickly nodes move, the higher weight the mobility cost has. Further, $C_M^{\ell_{u,v}}$ is a main factor in $C_{M+I}^{\ell_{u,v}}$ when the maximal speed of mobile nodes is larger than 20 m/s under the condition $\beta = 1$. So, α can be set as $\alpha \ge 2$ when $V_{max} > 20$ m/s; otherwise, $\alpha \le 1$.

4.3 Channel Assignment

Our channel assignment avoids the impact to any PN and minimizes the interference to CNs located in a k-hop neighborhood, making full use of both *channel diversity* and *spatial reusability*.

4.3.1 Interference Avoidance to Primary Nodes

A CN v potentially impact a set of PNs, which we define as a potential conflict set (CS_v), i.e., $CS_v = \{PN_m | d_{v,PN_m}(t) \le R_I$ AND PN_m is *active*$\}$ at a time slot t. More specifically, any PN_m is added into CS_v only if $MLT_{u,v} \ge MLT_{v,PN_m}$ and PN_m is using its licensed channel c_{PN_m}.

A CN v only can use channels in its *available channel set* $ACS_v = C_v(t) \setminus \{c_{PN_m} | \forall PN_m \in CS_v\}$. In the case that $ACS_v = \Phi$, our J-SRCA sets $C_{I:PN}^{\ell_{u,v}} = \infty$ so that the $IDTC_{f_k}^{\ell_{u,v}}$ becomes infinite and accordingly, the node v will be excluded from the route selection.

4.3.2 Channel Assignment Algorithms

Channel assignment algorithms select an available channel for the next-hop candidate v and calculate $C_I^{\ell_{u,v}}$. They are called by our J-SRCA, described in Section 4.4, according to v's *node types* (*normal* and *critical nodes*) and *interference categories* (*DJFI* and *JFI*).

(1) *CANN*. It assigns a channel for a *normal node* that only interferes with the last k upstream links in an intra-flow. Algorithm 1 (*CANN*) describes how to assign a channel $c_{u,v}$ to $\ell_{u,v}$ in f_i for a normal node v. In *CANN*, $c_{x-hop}^{f_i}$ refers to the channel assigned to the link $\ell_{x-hop}^{f_i}$, which is the x-hop upstream link away from $\ell_{u,v}$ in f_i. If a normal node does not have x-hop ($1 \le x \le k$) upstream node, $c_{x-hop}^{f_i}$ is set as ϕ. We always select the channel with a minimal sequence number from available channel set C, using $arg_{min} C$, to improve the channel reusability.

Algorithm 1 *CANN*.

1: Set up CS_u and CS_v according to Section 4.3.1;
   $ACS_u = \& C_u(t) \setminus \{c_{PN_m} | \forall PN_m \in CS_u\}$;
   $ACS_v = \& C_v(t) \setminus \{c_{PN_m} | \forall PN_m \in CS_v\}$;
2: if$(ACS_v = \Phi)\{C_{I:PN}^{\ell_{u,v}} = \infty;$ goto step 6;$\}$ else $C_{I:PN}^{\ell_{u,v}} = 0$;
3: $C_{u,v} = ACS_u \cap ACS_v$;
4: $C_{available} = C_{u,v} - \bigcup_{x=1}^{k} \{c_{x-hop}^{f_i}\}$;
5: if $(C_{available} \ne \Phi)\{c_{u,v} = arg_{min} C_{available}; C_{I:CN}^{\ell_{u,v}} = 0;\}$ else
   $\{c_{u,v} = arg_{\min} C_{u,v};\ C_{I:CN}^{\ell_{u,v}} = 1;\}$
6: $C_I^{\ell_{u,v}} = C_{I:PN}^{\ell_{u,v}} + C_{I:CN}^{\ell_{u,v}}$;

The first three steps in *CANN* calculates the common available channel set $C_{u,v}$. The step 4 excludes channels that have been assigned to the last k upstream hops in f_i from $C_{u,v}$. If $C_{available} \ne \Phi$, $\ell_{u,v}$ will be assigned a channel with minimal number from $C_{available}$ in step 5. In this case,

we set up $C_{I:CN}^{\ell_{u,v}} = 0$ because $\ell_{u,v}$ does not interfere with the intra-flow f_i. Otherwise, there is an intra-flow interference and we set $C_{I:CN}^{\ell_{u,v}} = 1$.

(2) *CACrN*. Algorithm 2 (*CACrN*) assigns a channel for a *critical node* that interferes with both intra- and inter-flows. Similar to Algorithm 1, the first three steps in the Algorithm 2 avoid the channel conflict to PNs. The following steps in *CACrN* guarantees that $c_{u,v}$ does not interfere links within k hops away from $\ell_{u,v}$ in all inter-flows f_j $(j = 1, 2, \ldots, K; j \neq i)$, i.e., the black square nodes in our interference graph in Fig. 2. $C_{available}$ in *CACrN* depends on interference categories.

- In case that f_j is a JFI-interference inter-flow,

$$C_{available} = C_{u,v} - \bigcup_{j} \bigcup_{x=1}^{k} \left\{ c'^{f_j}_{x-hop}, c^{f_j}_{x-hop} \right\}.\ c^{f_j}_{x-hop}$$

  $(c'^{f_j}_{x-hop})$ denote a channel assigned to $\ell^{f_j}_{x-hop}$ $(\ell'^{f_j}_{x-hop})$ that is x-hop away from v in s_j (d_j) side in f_j.
- In case that f_j is a DJFI-interference inter-flow,

$$C_{available} = C_{u,v} - \bigcup_{j} \bigcup_{x=2}^{k} \left\{ c'^{f_j}_{x-hop}, c^{f_j}_{x-hop} \right\}.$$

Algorithm 2 *CACrN*.

1: The first three steps are similar to those in *CANN*
2: $C_{available} = C_{u,v} - \bigcup_j \{c^{f_j}_{x-hop} | \ell^{f_j}_{x-hop}$ is within k hops from $\ell_{u,v}\}$;
3: if $(C_{available} \neq \Phi)$
  if $(C_{available} - \bigcup_{x=1}^{k} \{c^{f_i}_{x-hop}\}) \neq \Phi)\{c_{u,v} = arg_{\min}$ $(C_{available} - \bigcup_{x=1}^{k} \{c^{f_i}_{x-hop}\}); C_{I:CN}^{\ell_{u,v}} = 0;\}$
  else $\{c_{u,v} = arg_{\min} C_{available};\ C_{I:CN}^{\ell_{u,v}} = 1;\}$
 else $\{C_{I:CN}^{\ell_{u,v}} = \xi;$
  if $(C_{u,v} - \bigcup_{x=1}^{k} \{c^{f_i}_{x-hop}\}) \neq \Phi)$
   $\{c_{u,v} = arg_{\min}(C_{u,v} - \bigcup_{x=1}^{k} \{c^{f_i}_{x-hop}\};\}$
  else $\{c_{u,v} = arg_{\min} C_{u,v};\ C_{I:CN}^{\ell_{u,v}} = C_{I:CN}^{\ell_{u,v}} + 1;\}\}$
4: $C_I^{\ell_{u,v}} = C_{I:PN}^{\ell_{u,v}} + C_{I:CN}^{\ell_{u,v}}$;

Note that *CACrN* sets $C_{I:CN}^{\ell_{u,v}} = 1$ if $\ell_{u,v}$ interferes with only an intra-flow f_i. When $\ell_{u,v}$ interferes with an inter-flow f_j, however, its channel interference cost is added ξ $(\xi > 1)$ through $C_{I:CN}^{\ell_{u,v}} = \xi$ so that a candidate v with the inter-flow interference has a lower probability to be selected as the next hop than the node with only the intra-flow interference.

4.4 Joint Stable Routing and Channel Assignment (J-SRCA)

4.4.1 Geography-Based Routing Mechanism

Our J-SRCA employs on-demand routing mechanism due to the node mobility, which in general introduces the flooding. To reduce routing overhead, we make full use of geography information, like the proposals in [9], [10]. Specifically, our J-SRCA selects the next hop only within a controlled sector region with an angle φ towards the destination. The sector is circled at a relay u with a radius R_T, which is illustrated in Section 1 of the supplementary which is available in the Computer Society Digital Library at http://doi.ieeecomputersociety.org/10.1109/TPDS.2013.216.

To control the path length, we initially set $\varphi = 90°$. The working node u, however, possibly cannot find any next hop v because there is no node located in the sector region with the angle $\varphi = 90°$. In this case, the J-SRCA will enlarge the sector region to a larger angle $\varphi + \Delta\varphi$ (e.g., 30°) step by step until it can find out the next hop. Note that each node can detect its location and velocity by a GPS device, and can query the location, velocity and available channels of its 1-hop neighbors, as well as channel status of k-hop neighboring nodes through an extended beacon mechanism.

We employ the location query service to acquire the geography information of destination nodes. A network is divided into a set of equivalent grids. A grid roughly covers the transmission range of a CN. All nodes register their location information in the well-know location server and autonomously update the information when they move out of its current grid. Before a source node initiates a route setup, it firstly queries the location server to determine location of the destination. Then, during route setup and data transmission, each node in the selected path appends its current location in routing and data packets. Especially, when a relay finds its next hop becomes unavailable during a data transmission, it initiates our *Local Route Recovery* process, described in the following, to maintain the path using the geography information contained in data packets.

4.4.2 Hop-By-Hop Route Setup

J-SRCA protocol is initiated by a source node s_k and is executed hop by hop. The working node u that is running J-SRCA directly determines the next hop v based on the lowest $IDTC_{f_k}^{\ell_{u,v}}$ until $v = d_k$.

1) *Joint next-hop selection and channel assignment*. A working node u calculates the *IDTC* of each neighboring node located in the sector region based on our transmission cost model, where it calls our channel assignment algorithms to estimate the channel interference cost. Based on the transmission cost estimation, u selects the node $v \in N^u$ with the lowest $IDTC_{f_k}^{\ell_{u,v}}$ as the next hop, and at the same time assigns a channel $c_{u,v}$ to $\ell_{u,v}$. Then, u sends a *route selection and channel assignment packet (RSCAP)* to v. Main fields in the RSCAP packet include *unique packet ID, unique flow ID, 2-dimension node coordinate, selected sub-path*$P_{s_k}^u$, *assigned channel*$c_{u,v}$, *sender and destination*. Once receiving the RSCAP packet, v becomes a new working node and it in turn runs J-SRCA protocol and sends the updated RSCAP packet to its next hop. Algorithm 3 describes the J-SRCA, where the sub-path $P_{s_k}^u$ is cumulated hop by hop and becomes a complete path $P_{s_k}^{d_k}$ when J-SRCA stops due to $v = d_k$. Note that $P_{s_k}^u = \Phi$ when s_k initiates the J-SRCA.

Algorithm 3 J-SRCA.

1: $IDTC[u] = \infty$;
2: identify set V of nodes in sector with an angle φ;
3: **while**$(V \neq \phi)$**do**
4: set v as the first element in V;

5: calculate mobility cost $C_M^{\ell_{u,v}}$ using formula (14);
6: call CANN (CACrN) to estimate interference cost $C_I^{\ell_{u,v}}$ based on node type of v;
7: $IDTC_{f_k}^{\ell_{u,v}} = (C_M^{\ell_{u,v}} + \alpha C_I^{\ell_{u,v}}) \times (1 + \frac{b_v^c}{B_v^c}) \times \frac{d_{v,d_k}}{d_{u,d_k}}$;
8: if $(IDTC_{f_k}^{\ell_{u,v}} < IDTC[u])$

$$\left\{ IDTC[u] = IDTC_{f_k}^{\ell_{u,v}}; \quad \mu = v; \right\}$$

9: $V = V - v$;
10: **end while**
11: if ($IDTC[u]$ is still ∞) $\{\varphi = \varphi + \Delta\varphi$; go to step 3$\}$
12: $P_{s_k}^u = P_{s_k}^u + \mu$;
13: update RSCAP with $P_{s_k}^u$ and $c_{u,\mu}$, and send it to μ;

2) *Acknowledging selected route and assigned channels*. A RSCAP packet is transferred hop by hop towards to the destination d_k. When the RSCAP packet reaches d_k, d_k gets both the stable route $P_{s_k}^{d_k}$ and assigned channels $C_{s_k}^{d_k}$ for each link in $P_{s_k}^{d_k}$. So, d_k immediately responds a *route and channels response packet* (*RCRP*) that includes $P_{s_k}^{d_k}$ and $C_{s_k}^{d_k}$ to s_k via the inverse path of $P_{s_k}^{d_k}$. On receiving *RCRP* packet, s_k starts transmitting f_k through $P_{s_k}^{d_k}$ on $C_{s_k}^{d_k}$.

4.4.3 K-Hop Channel Adjustment

In the following two cases, channels need to be further adjusted to improve the network performance.

1) *Channel adjustment* during a channel assignment due to insufficient available channels in working node u. Since our approach gives higher priority to avoiding inter-flow channel conflict, a link may conflicts with the last k upstream links even the latter has other available channels. As shown in Fig. 3, e.g., we are assigning channels for f_i while f_j is an existing inter-flow. The first three links of f_i have been assigned channels c1, c2, and c3, respectively. When C runs J-SRCA to assign a channel for $\ell_{C,E}$, however, it has to choose c3 to avoid the interference with $\ell_{H,I}$ and $\ell_{I,J}$ in f_j, where we let k=2 in the interference model for the simplicity. Unfortunately, c3 interferes with $\ell_{B,C}$. In this case, we adjust assigned channels within k upstream links in f_i. For the scenario in Fig. 3, channels for last upstream links are jointly adjusted as $c_{C,E} = 3$, $c_{B,C} = 2$, and $c_{A,B} = 5$ so that all interferences can be avoided.

2) *Channel switch* during a data transmission due to PN activation. When a PN_m with a licensed channel c_m activates during data transmission, the link that was assigned c_m has to switch to another orthogonal channel c_n. c_n should not interfere with inter-flow(s) f_j and intra-flow f_i. Let links $\ell_{C,E}$, $\ell_{B,C}$ and $\ell_{A,B}$ in Fig. 3 be assigned channels 3, 2 and 5 respectively. PN_5, which locates in R_I of $\ell_{A,B}$, starts communicating during the f_i's transmission. In this case, we adjust channels of $\ell_{A,B}$ from $c_{A,B} = 5$ to $c_{A,B} = 1$. Subsequently, the channel of $\ell_{s_i,A}$ will be switched from $c_{s_i,A} = 1$ to $c_{s_i,A} = 6$.

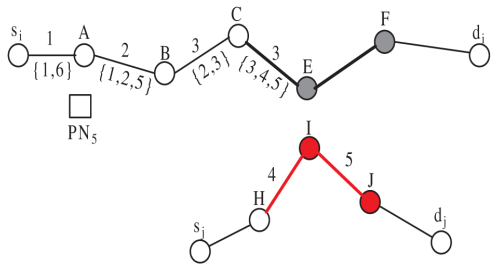

Fig. 3. Channel adjustment.

4.4.4 Local Route Recovery

A (or more) link(s) $\ell_{u,v}$ in a selected route may become unavailable during a data transmission due to $d_{u,v}(t) > R_T$ or node crash. In AODV [11], once a link becomes broken, the link failure message is sent back to the source node and the latter restarts the discovery process to set up a new route. This policy loses packets on the way and spends an extra time on new route setup. Instead, we use a two-hop local route recovery mechanism.

1) *Link failure detection*. We assume that nodes use 802.11 MAC protocol, in which a sender u will retransmit a data frame if it does not receive an ACK from the receiver v within a specified interval. We use the timeout mechanism to detect the link failures. Specifically, if u does not receive an ACK after r times (e.g., r = 3) of retransmission, it makes a decision that $\ell_{u,v}$ is unavailable.

2) *Two-hop local path maintenance*. In the routing response process, each node in $P_{s_k}^{d_k}$ records the whole path from s_k to d_k. Once u detects $\ell_{u,v}$ becomes unavailable, it initiates a local routing process to find a sub-path from u to v' next hop (i.e., node A in Fig. 4). On receiving *RCRP* packet from A, remaining data will be transmitted over a new route (i.e., $\ldots \rightarrow u \rightarrow x \rightarrow A \rightarrow \ldots$). Otherwise, u will try again to set up a sub-path to B (the second hop of v). In most of link failures, our J-SRCA can success on one-hop sub-path (i.e., $P_u^A = \langle u, x, A \rangle$ in Fig. 4) maintenance in our experiments. In the worst case that two-hop local sub-path (i.e, P_u^B) can not be set up, u finally reports a link failure message to s_k. s_k reconstructs a totally new route between s_k and d_k.

5 Performance Evaluation

We developed a simulation system, which is built on the NS2 simulator [19] with multi-radio multi-channel extensions, to comprehensively evaluate our J-SRCA protocol.

5.1 System Setup

PNs and CNs are randomly deployed and move at a speed randomly distributed in [0, $V_{\max}$]. Channels comply with the Two-Way Rayleigh model. Signal propagation

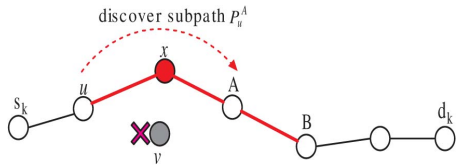

Fig. 4. Local recovery.

TABLE 2
System Parameters

Parameters	*Values*
Transmission range (R_T)	125m
Interference range (R_I)	250m
Packet size (S_{packet})	512KB
Number of totally available channels	15
Number of CN (N)	200
Number of PN (M)	20
Maximal speed (V_{max})	10m/s
Number of data flows (K)	5

was set as Two-Ray Ground Reflection model. PNs and CNs have the same transmission radius and interference range. Each PN is assigned a fixed data channel and randomly uses it.

All CNs share the same common control channel. Each CN has multiple available data channels. In the experiments, we tested different performance metrics for 500 s. Each flow is generated through NS2-based FTP data generator and transferred through a TCP connection. Other parameters are listed in Table 2.

5.2 Performance Evaluation

We evaluate our J-SRCA protocol through comparing it with the following related protocols.

- *PCTC* [7]. It is the most related to our J-SRCA. PCTC selects the path with maximum duration to mitigate rerouting frequency for performance improvement, based on the link-availability prediction. Any pair of neighboring nodes in a path randomly selects a common channel for the data transmission.
- *AODV* [11]. This protocol is extended for multi-channel environments. It selects a path with the least latency. Also, links in a path randomly use available channels.
- *SR* (stable routing). This is only the routing scheme of our J-SRCA. *SR* selects routes only in terms of our link stability prediction model.

We use the following six performance metrics to evaluate the above solutions.

5.2.1 Aggregated System Throughput (AST)

We use the *aggregated system throughput* (*AST*), which is the sum of concurrent data flows, to compare the parallel transmission ability of our J-SRCA with the most related PCTC in the following scenarios.

(1) *Concurrent Data Flows.* With the increase of concurrent data flows (K), AST in J-SRCA and PCTC grows up, but with very different growth rate. Fig. 5a shows that our J-SRCA outperforms PCTC. In particular, when K increases up to 4, the AST in PCTC has little increase while our J-SRCA still exhibits significant improvements. PCTC performs a low throughput because it excludes the nodes moving towards to any PN even the latter has other orthogonal channels during its topology construction and route selection. What is more important is that more

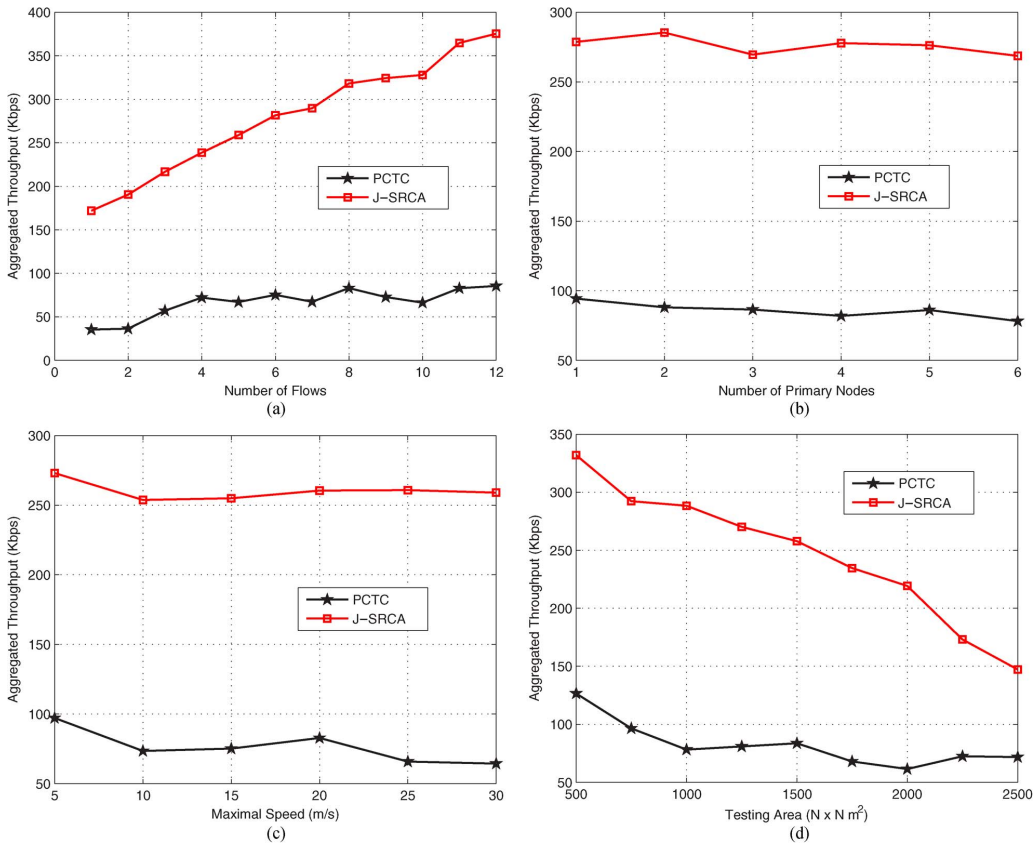

Fig. 5. Aggregated system throughput. (a) Number of flows. (b) Number of primary nodes. (c) Maximal speed. (d) Network area.

concurrent flows cause more serious channel interference in PCTC, while J-SRCA can significantly mitigate the channel interference.

(2) *Primary Nodes.* More PNs potentially make routes more instable because some CNs have to give up the channels being occupied by PNs. Fig. 5b, however, demonstrates the significant improvement of our J-SRCA, compared with PCTC. The high throughput of J-SRCA in face of unexpected PNs results from flexible channel assignment. Firstly, if a PN is active during a route setup, our J-SRCA can select other unused channels. On the other hand, when any PN_m reactivates during a data transmission, the link that was assigned the channel c_{PN_m} can switch to another channel using our *k-Hop Channel Adjustment* mechanism. As a result, our J-SRCA almost does not suffer from the increase of PNs in terms of the AST.

(3) *Node Mobility.* As shown in Fig. 5c, PCTC exhibits a low throughput while our J-SRCA has a relatively stable throughput under high mobility. The reason is our J-SRCA jointly selects a stable next hop and assigns a interference-free channel which PCTC lacks flexible channel assignment.

(4) *Network Area.* With the increase of the network area, the AST in J-SRCA and PCTC degrades, as shown in Fig. 5d. The reason is that the more the network area is, the lower the CN density become and accordingly, the lower the average duration of each link become. The J-SRCA, however, significantly outperforms PCTC because J-SRCA jointly selects the stable route and mitigates co-channel interference.

5.2.2 Average End-to-End Delay

Network latency is important to delay-sensitive applications [12]. We evaluated the *average end-to-end delay* of all the solutions, which represents the average duration from sending a packet in a source node to receiving the packet in the destination node. The following results demonstrate how the average end-to-end delay in the four solutions changes in different scenarios.

Average delay in AODV, SR and PCTC have higher growth with the number of flows than that in J-SRCA, as shown in Figs. 6a and 7a. The main reason is that the J-SRCA assigns orthogonal channels to avoid channel conflict during route setup and can adjust channel if a PN reactivates during data transmission. Instead, AODV, SR and PCTC lack of flexible channel assignment and channel adjustment, which results in more data retransmissions.

When PNs start employing their channel, adjacent CNs using these licensed channels have to give up the transmission in AODV, SR, and PCTC, which causes longer delay, illustrated in Figs. 6b and 7b. From Fig. 6b, we also can see that AODV causes an increasing end-to-end delay with more PNs. Note that PCTC exhibits a better performance in network delay than AODV because PCTC always selects CNs away from any PN. Our J-SRCA, however, has a much lower and stable delay with the

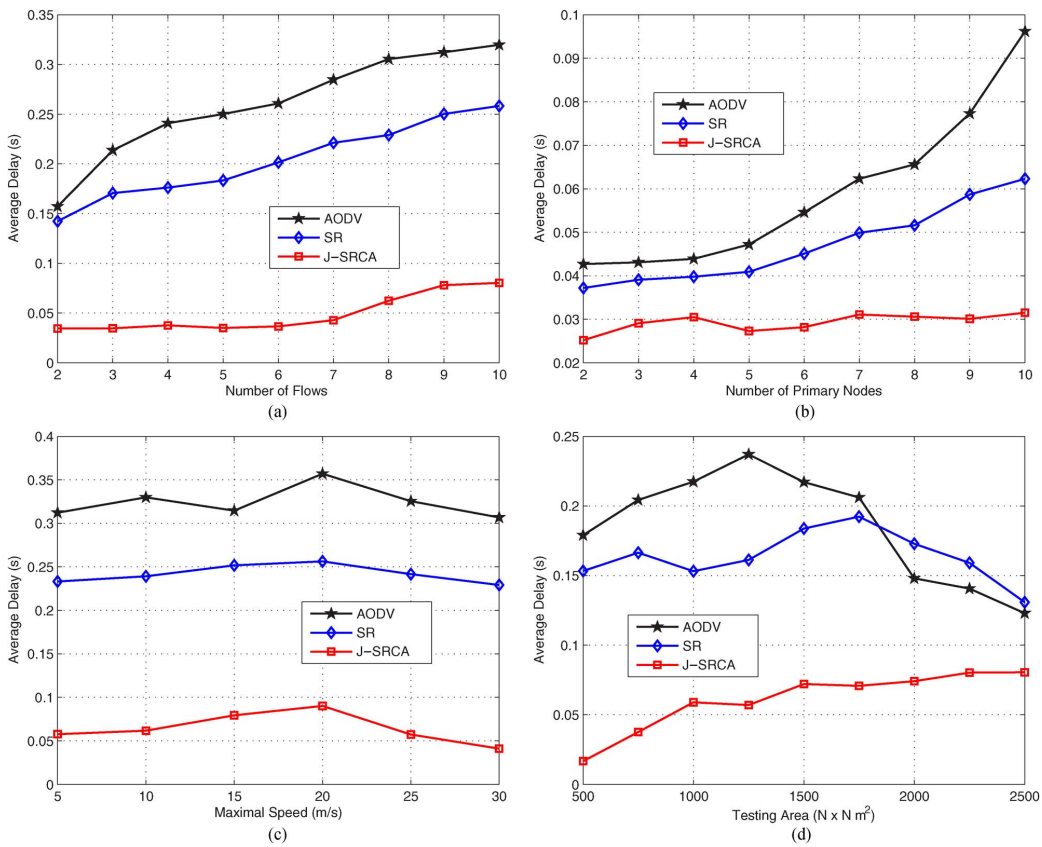

Fig. 6. Average end-to-end delay in different scenarios. (a) Number of flows. (b) Number of primary nodes. (c) Maximal speed. (d) Network area.

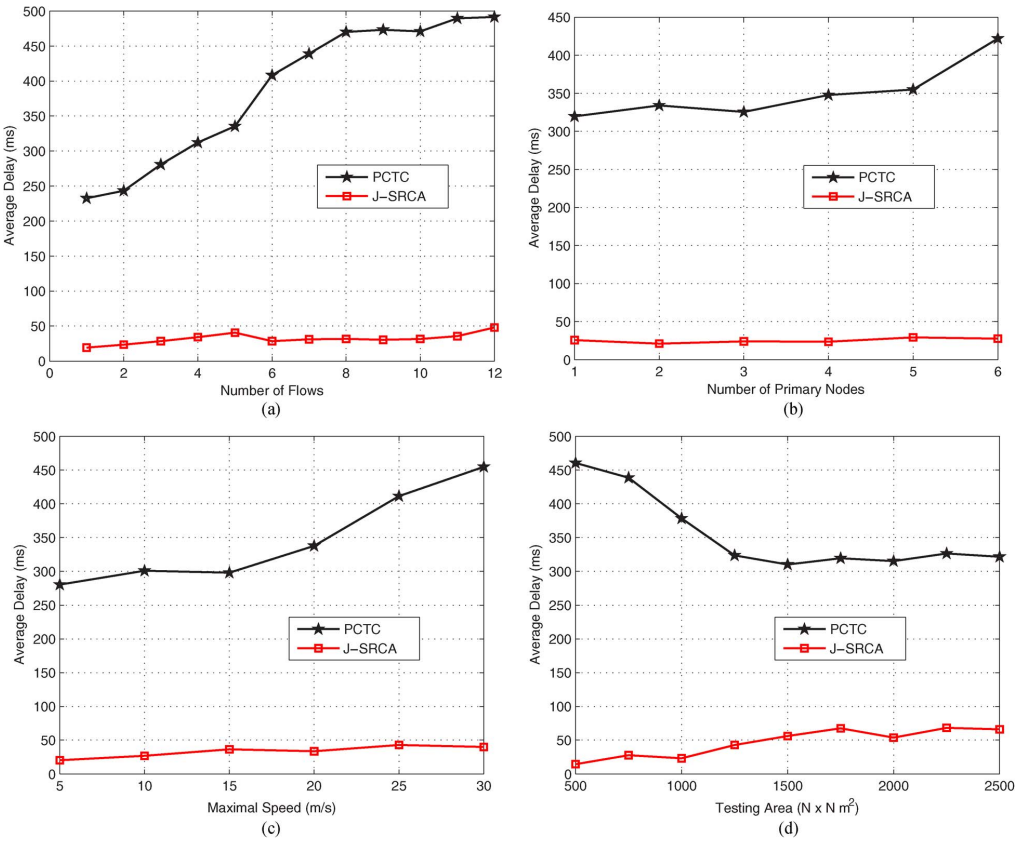

Fig. 7. Delay comparison between J-SRCA and PCTC. (a) Number of flows. (b) Number of primary nodes. (c) Maximal speed. (d) Network area.

increase of PNs. The main reason is that our J-SRCA always avoids using the paths and channels that interfere with PNs.

Node mobility also affects network delay. Figs. 6c and 7c show that for all protocols, the delay increases with the maximal speed. This is because higher speed leads to more data retransmission even reconstruction of the whole route. Nevertheless, our J-SRCA exhibits the best performance in network delay. The reason is that J-SRCA always selects stable links and assigns the interference-avoiding channels, together with a channel adjustment mechanism during data transmission.

With the increase of network area, PCTC, AODV and SR exhibit higher average delay than the J-SRCA, as shown in Figs. 6d and 7d. An interesting phenomenon is that average delay in AODV drops when network area is larger than 1250 m $\times$ 1250 m, which is caused by the fact that with the increase of network area, AODV averagely needs less hops for a data transmission session. Note that our average end-to-end delay metric only covers the packets received successfully by their destination nodes.

5.2.3 Packet Loss Ratio (PLR)

We define the packet loss ratio (*PLR*) as the rate of all the dropped packets in the network to the total packets sent from all source nodes during the given testing period.

The experimental results show that the PLR in all the solutions grows up as the number of flows increases. Fig. 8a, however, reveals that the J-SRCA has a lower PLR than AODV and SR. The reason is that our J-SRCA can mitigate the interference through assigning channels in the interference-avoiding way. Next, from Fig. 8b, we can find that J-SRCA has a relatively stable PLR while PLR in both AODV and SR significantly grows up with more PNs. The reason is that our J-SRCA can find an available channel different from the ones licensed for *potential conflict primary nodes* for each link. Instead, AODV and SR have to give up data transmission when CNs move to the R_I of potential conflict primary nodes.

Higher node mobility results in more packet loss due to more route failures, demonstrated in Fig. 8c. J-SRCA, however, has a significant improvement because it experiences much less route failures than AODV. Moreover, PLR in SR is always higher than that in J-SRCA because SR suffers from more channel conflicts. Finally, with the increase of network area, average distance between CNs becomes longer. As a result, the duration of links significantly decreases and routes need to be reconstructed more often, resulting in higher PLR, shown in Fig. 8d. Our J-SRCA, however, still outperforms over AODV and SR in terms of the PLR.

5.2.4 Routing Overhead (RoH)

We also use routing overhead (*RoH*), which is the ratio of the number of routing packets to the number of both routing and data packets, to evaluate the efficiency of our J-SRCA for route setup. From Fig. 9, we can find that our J-SRCA and SR have much lower routing overhead than AODV under not only more flows and PNs but also higher mobility and lager network area. The reason is

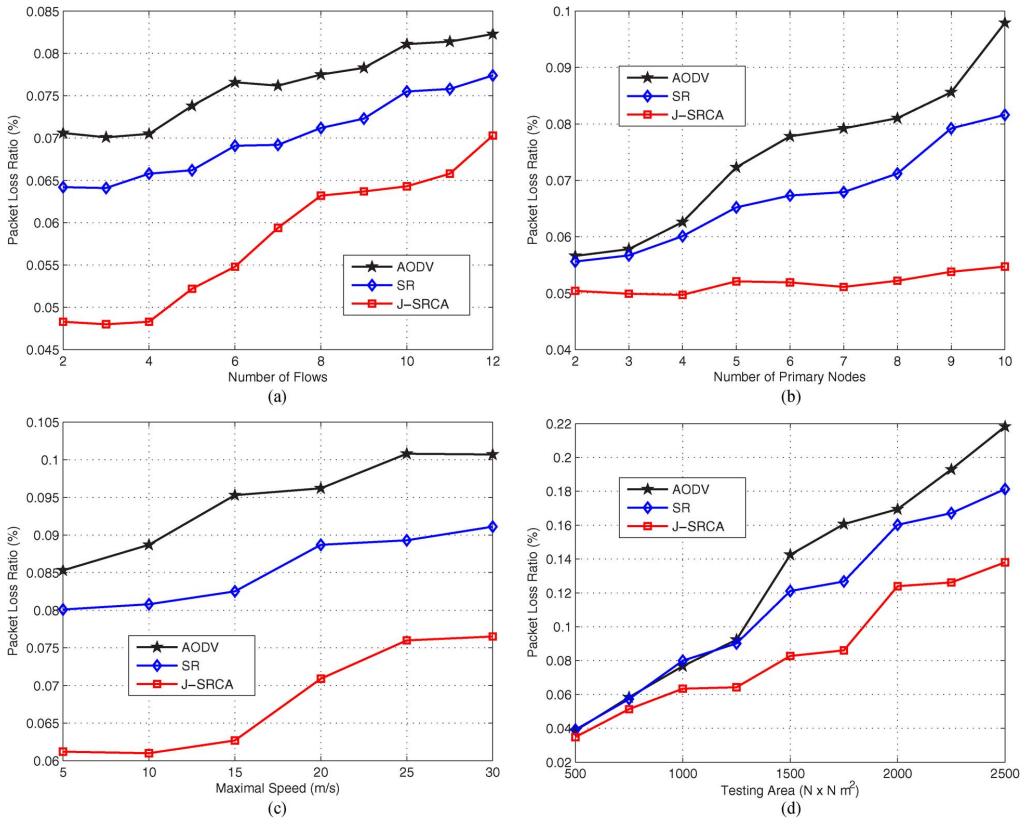

Fig. 8. Packet loss ratio in different scenarios. (a) Number of flows. (b) Number of primary nodes. (c) Maximal speed. (d) Network area.

that both J-SRCA and SR select stable routes which can keep a longer duration while AODV needs more routing reconstruction. In any case, J-SRCA outperforms a little than SR because the SR often has to abandon routes due to the appearance of PNs. On the other hand, *RoH* in AODV drops when network area is lager than 1000 m $\times$ 1000 m, as shown in Fig. 9d. It results from the fact that the CN density become low when the network area exceeds 1000 m $\times$ 1000 m, and as a consequence, many flooding messages are lost because many CNs cannot directly communicate. In other words, sparse node density limits many flooding packets so that there are relatively less routing packets during a route setup under lager network area.

5.2.5 Average Path Duration

To verify the path stability of our approach, we tested and compared the path duration among J-SRCA, PCTC and AODV, where paths selected by the three protocols were set the same source and destination nodes. In this paper, the path duration D_p refers to the interval from the end of route setup to the time whenever any link becomes broken. Essentially, D_p is the lifetime of the most instable link such that $D_p = \min\{D_{\ell_i}\}$, where D_{ℓ_i} is the duraiton of any link ℓ_i in the selected path.

Path duration is greatly dependent on node mobility and network size. The results in Fig. 10 illustrates that our J-SRCA performs longer path duration than PCTC and AODV. So, paths selected by our J-SRCA is more stable than that by PCTC and AODV because the J-SRCA not only chooses the stable links, but also flexibly assigns and adjusts channels.

5.2.6 Average Path Length

For a pair of specified source and destination nodes, too many hops between them generally degrade network performance. The path length refers to hops in the paths selected by the three protocols, with the same source and target nodes in our experiments. We tested average path length in the J-SRCA, AODV and PCTC.

As illustrated in Fig. 11, our J-SRCA exhibits only more 8 percent average hops than AODV and less average hops than PCTC. AODV protocol in general selects the shortest path. So, our J-SRCA does not introduce more hops, compared with AODV and PCTC. The reason is that during route setup, our J-SRCA selects the next relay within a controlled sector towards the specified destination.

Based on the above experimental results, we can conclude that our J-SRCA is able to adapt well to mobile cognitive networks.

6 Related Work

Most related researches focus on *static networks* [4], [9], [13], [14], [15]. Although other proposals were designed for *mobile networks*, they either do not consider channel vacation to PNs, or set up routes and assign channels separately [16], [17], [18]. Moreover, interference graph also was researched by related work [19], [20]. Details can be found in Section 2 of the supplementary available online.

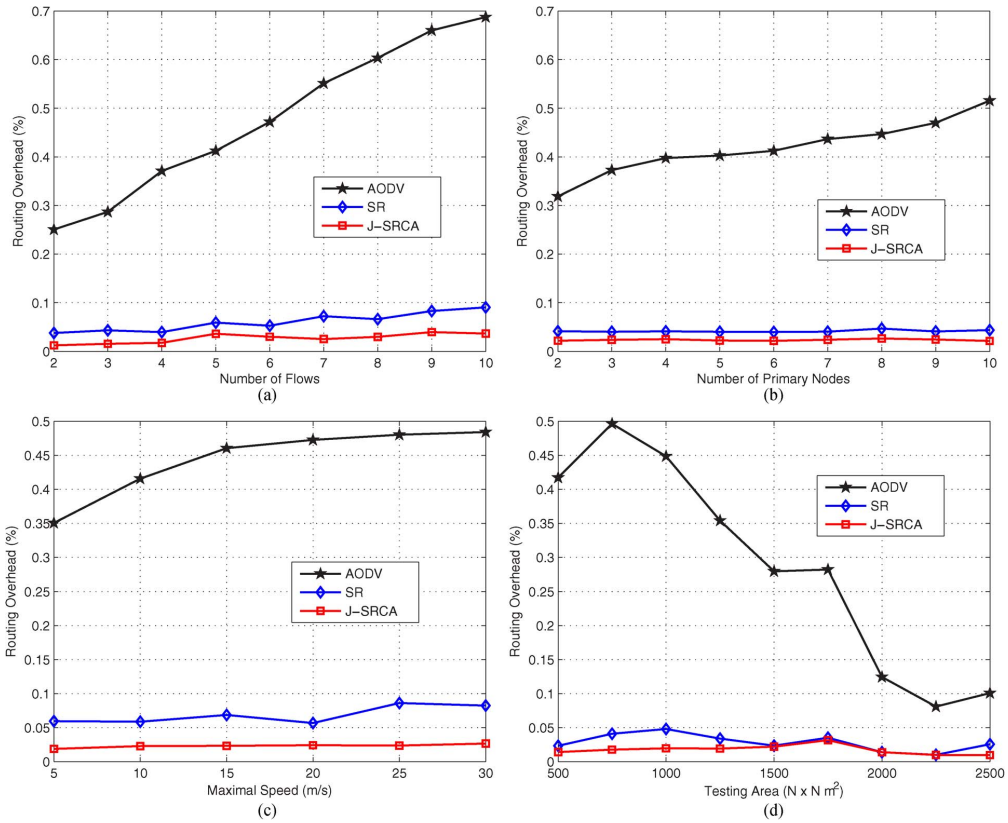

Fig. 9. Routing overhead in different scenarios. (a) Number of flows. (b) Number of primary nodes. (c) Maximal speed. (d) Network area.

7 Conclusion and Future Work

We presented the J-SRCA protocol that jointly selects stable route and assigns interference-avoiding channels for MACNets. Firstly, we developed a transmission cost metric *IDTC* that captures the link stability, channel interference with PNs and CNs, node workload and path length. We, then, proposed the interference graph for efficient channel assignment and designed channel assignment algorithms. Finally, we proposed the J-SRCA protocol. Advantages over existing works, our approach jointly optimizes route stability and channel assignment based on the mobility prediction. Comprehensive experiment results demonstrate that our J-SRCA significantly improves various network performances, especially in face of *more primary nodes* and *higher node mobility*. As a part of our future work, we are going to investigate how to theoretically analyze and proof J-SRCA problem and further optimize the solution.

Acknowledgment

This work was supported by the National Natural Science Foundation of China (NSFC) projects (Nos. 91438121, 61373156, 61272442 and 61073148), the Key Basic Research Project (No. 12JC1405400) and the Shanghai Pujiang Program (No. 13PJ1404600) of the Shanghai Municipality,

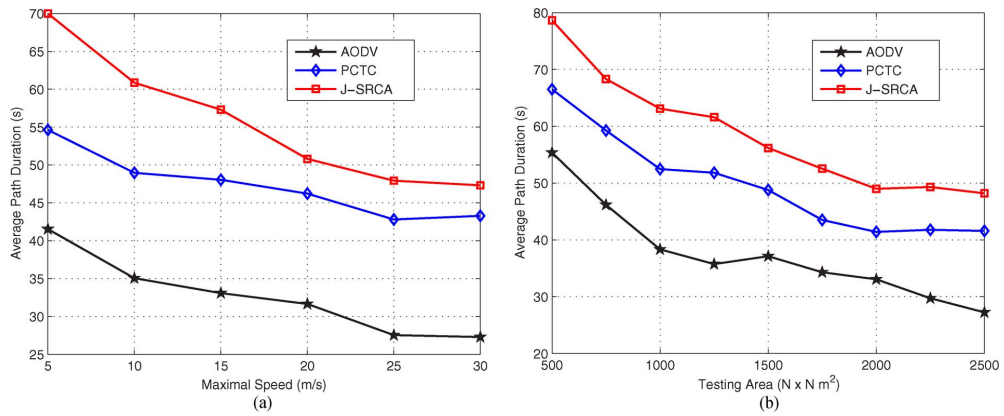

Fig. 10. Average path duration. (a) Maximal speed. (b) Network area.

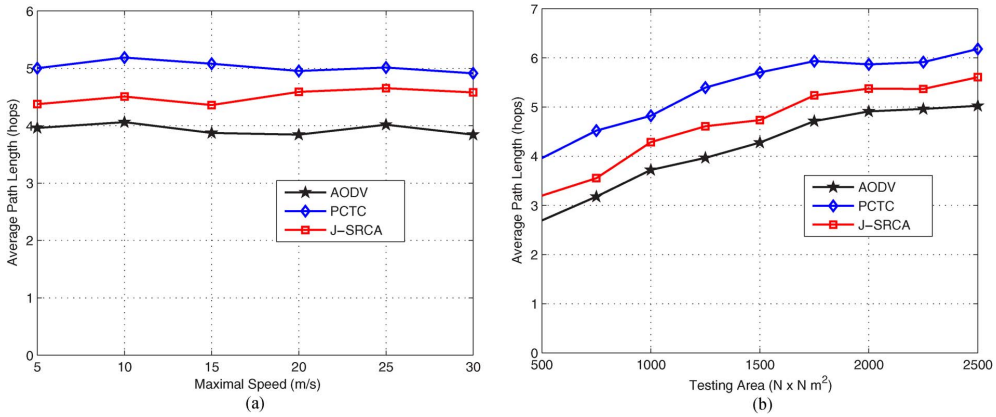

Fig. 11. Average path length. (a) Maximal speed. (b) Network area.

the National Basic Research Program (973 Program, No. 2015CB352400), Huawei Projects (Nos. YB2015090040, and YB2015080089) and Shanghai Branch of Southwest Electron and Telecom Technology Research Institute Project (No. 2013008).

REFERENCES

[1] I.F. Akyldiz and W. YLee, ''A Spectrum Decision Framework for Cognitive Radio Networks,'' *IEEE Trans. Mobile Comput.*, vol. 10, no. 2, pp. 161-174, Feb. 2011.
[2] A. Abbagnale and F. Cuomo, ''Gymkhana: A Connectivity-Based Routing Scheme for Cognitive Radio Ad Hoc Networks,'' in *Proc. IEEE INFOCOM*, 2010, pp. 1-5.
[3] K.R. Chowdhury and M.D. Felice, ''SEARCH: A Routing Protocol for Mobile Cognitive Radio Ad-Hoc Networks,'' in *Proc. IEEE SARNOFF Symp.*, 2009, pp. 1-6.
[4] L. Chen, Q. Zhang, M.L. Li, and W.J. Jia, ''Joint Topology Control and Routing in IEEE 802.11-Based Multiradio Multichannel Mesh Networks,'' *IEEE Trans. Veh. Technol.*, vol. 56, no. 5, pp. 3123-3136, Sept. 2007.
[5] L.F. Lai, H.E. Gamal, H. Jiang, and H.V. Poor, ''Cognitive Medium Access: Exploration, Exploitation, Competition,'' *IEEE Trans. Mobile Comput.*, vol. 10, no. 2, pp. 239-253, Feb. 2011.
[6] G. Carofiglio, C.F. Chiasserini, M. Garetto, and E. Leonardi, ''Route Stability in MANETs Under the Random Direction Mobility Model,'' *IEEE Trans. Mobile Comput.*, vol. 8, no. 9, pp. 1167-1179, Sept. 2009.
[7] Q.S. Guan, F.R. Yu, S.M. Jiang, and G. Wei, ''Prediction-Based Topology Control and Routing in Cognitive Radio Mobile Ad Hoc Networks,'' *IEEE Trans. Veh. Technol.*, vol. 59, no. 9, pp. 4443-4452, Nov. 2010.
[8] S.M. Jiang, D.J. He, and J.Q. Rao, ''A Prediction-Based Link Availability Estimation for Routing Metrics in MANETs,'' *IEEE/ACM Trans. Netw.(TON)*, vol. 13, no. 6, pp. 1302-1312, Dec. 2005.
[9] B. Karp and H.T. Kung, ''GPSR: Greedy Perimeter Stateless Routing for Wireless Networks,'' in *Proc. MobiCom*, 2000, pp. 243-254.
[10] M. Zorzi and R.R. Rao, ''Geographic Random Forwarding (GeRaF) for Ad Hoc and Sensor Networks: Multihop Performance,'' *IEEE Trans. Mobile Comput.*, vol. 2, no. 4, pp. 337-348, Oct.-Dec. 2003.
[11] H. Nakayama, S. Kurosawa, A. Jamalipour, Y. Nemoto, and N. Kato, ''A Dynamic Anomaly Detection Scheme for AODV-Based Mobile Ad Hoc Networks,'' *IEEE Trans. Veh. Technol.*, vol. 58, no. 5, pp. 2471-2481, June 2009.
[12] Y. Ding and L. Xiao, ''Video On-Demand Streaming in Cognitive Wireless Mesh Networks,'' *IEEE Trans. Mobile Comput.*, vol. 12, no. 3, pp. 412-423, Mar. 2013.
[13] X.Y. Li, Y. Wang, H.M. Chen, X. Chu, Y.W. Wu, and Y. Qi, ''Reliable and Energy-Efficient Routing for Static Wireless Ad Hoc Networks With Unreliable Links,'' *IEEE Trans. Parallel Distrib. Syst.*, vol. 20, no. 10, pp. 1408-1421, Oct. 2009.
[14] A. Raniwala and T. Chiueh, ''Architecture and Algorithms for an IEEE 802.11-Based Multi-Channel Wireless Mesh Network,'' in *Proc. IEEE INFOCOM*, 2005, pp. 2223-2234.
[15] N. Devroye, P. Mitran, and V. Tarokh, ''Achievable Rates in Cognitive Radio Channels,'' *IEEE Trans. Inf. Theory*, vol. 52, no. 5, pp. 1813-1827, May 2006.
[16] M.X. Gong, S.F. Midkiff, and S.W. Mao, ''On-Demand Routing and Channel Assignment in Multi-Channel Mobile Ad Hoc Networks,'' *Ad Hoc Netw.*, vol. 7, no. 1, pp. 63-78, Jan. 2009.
[17] H.S. Chiu, K.L. Yeung, and K.S. Lui, ''J-CAR: An Efficient Joint Channel Assignment and Routing Protocol for IEEE 802.11-Based Multi-Channel Multi-Interface Mobile Ad Hoc Networks,'' *IEEE Trans. Wireless Commun.*, vol. 8, no. 4, pp. 1706-1715, Apr. 2009.
[18] A. Boukerche, A. Zarrad, and R.B. Araujo, ''A Cross-Layer Approach-Based Gnutella for Collaborative Virtual Environments Over Mobile Ad Hoc Networks,'' *IEEE Trans. Parallel Distrib. Syst.*, vol. 21, no. 7, pp. 911-924, July 2010.
[19] S.C. Liu, G.L. Xing, H.W. Zhang, J.P. Wang, J. Huang, M. Sha, and L.S. Huang, ''Passive Interference Measurement in Wireless Sensor Networks,'' in *Proc. IEEE ICNP*, 2010, pp. 52-61.
[20] J. Huang, S.C. Liu, G.L. Xing, H.W. Zhang, J.P. Wang, and L.S. Huang, ''Accuracy-Aware Interference Modeling and Measurement in Wireless Sensor Networks,'' in *Proc. ICDCS*, 2011, pp. 172-181.
[21] R. Vaze, ''Percolation and Connectivity on the Signal to Interference Ratio Graph,'' in *Proc. IEEE INFOCOM*, 2012, pp. 513-521.

Feilong Tang received the PhD degree in computer science from Shanghai Jiao Tong University (SJTU), China, in 2005. Currently, he is a Full Professor in the Department of Computer Science and Engineering of SJTU. In past years, he was a Japan Society for the Promotion of Science Postdoctoral Research Fellow in Japan and worked as Visiting Scholar at the Department of Computer Science of The University of Hong Kong for many years. His research interests focus on mobile cognitive networks, wireless sensor networks, algorithm design and evaluation and pervasive computing.

Minyi Guo received the PhD degree in computer science from University of Tsukuba, Japan. Currently, he is a Full Professor in the Department of Computer Science and Engineering, Shanghai Jiao Tong University, China. His research interests include pervasive computing, parallel and distributed processing, parallelizing compilers and software engineering. He is a Senior Member of the IEEE.

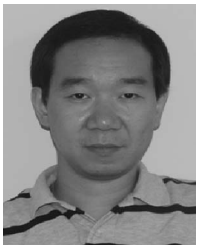

Song Guo received the PhD degree in computer science from the University of Ottawa, Canada in 2005. He is currently an Associate Professor in School of Computer Science and Engineering, the University of Aizu, Japan. His research interests are in the areas of protocol design and performance analysis for communication networks. He is a member of the IEEE.

Cheng-Zhong Xu received the PhD degree from the University of Hong Kong in 1993. He is a Full Professor in the Department of Electrical and Computer Engineering of Wayne State University (WSU) and Shenzhen Institutes of Advanced Technology, Chinese Academy of Sciences. His research interest includes networked computing systems and applications. He is an IEEE Fellow due to contribution in resource management in parallel and distributed computing.